Defect and Diffusion Forum Vols. 273-276 (2008) pp 643-648
online at http://www.scientific.net

Online available since 2008.02.11

Evaluation of the Coverage Pattern on the Fracture Surface of Bi-Embrittled Cu Grain Boundaries by Means of Auger Electron Spectroscopy

C.-H. Yeh[1,a], L.-S. Chang*[1,b] and B. Straumal[2,c]
[1]Department of Materials Engineering, National Chung Hsing University, 250 Kuo Kuang Road, 40227 Taichung, Taiwan/R.O.C.
[2]Institute of Solid State Physics, Russian Academy of Sciences, Chernogolovka, 142432 Moscow, Russia
[a]chyeh@dragon.nchu.edu.tw, [b]lschang@dragon.nchu.edu.tw, [c]straumal@issp.ac.ru

Abstract. In studying grain boundary segregation in Cu–Bi alloys by means of Auger electron spectroscopy samples must be broken *in-situ*. Consequently, the distribution of segregants on both sides of fracture path must be considered quantitatively. This question can be addressed by studying the influence of an adsorbed oxygen layer on the intensity of Auger peaks. This oxygen layer forms on the fracture surface when it is intentionally exposed to air. In this work, the values of Bi coverage have been measured both on the as-fractured Cu fracture surface and on the fracture exposed to air. The coverage values evaluated from the model of a crosstie-like pattern agree better with each other than those from the model of a continuous layer. Our study reveals that the Cu-Bi bond is weaker than the Bi-Bi bond.

INTRODUCTION

The grain boundary (GB) segregation in Cu–Bi alloys is well known and has been frequently investigated by Auger electron spectroscopy (AES) [1] and transmission electron microscopy (TEM) [2]. The amounts of segregation estimated from these two methods are comparable. Generally, a continuous layer of the segregating Bi is observed in TEM investigations. However, the AES sample must be broken *in-situ* to reveal GBs. Therefore, for the accurate quantification of GB Bi enrichment the question that has to be answered is how do segregated elements distribute between both sides of the fracture path.

The fracture path of Bi-embrittled grain boundaries in polycrystalline Cu depends on the strength of interatomic bonds at the interface. A continuous coverage of Bi atoms on Cu grain boundaries occurs if the Bi-Bi bond is weaker than the Cu-Bi bond. If the Cu-Bi bond is the weaker, a crosstie-like pattern is expected. The schemes of both coverage patterns are drawn in Figure 1. It is believed that the fracture of Bi-embrittled Cu grain boundaries belongs to the latter case. However, to the best of our knowledge, no evidence has been obtained previously.

In this work, the characteristic equations of Auger signals in the framework of a multilayer surface structure both for the crosstie-like and continuous coverage patterns were applied to fit the data in Auger electron spectra. The validities of these two patterns were compared.

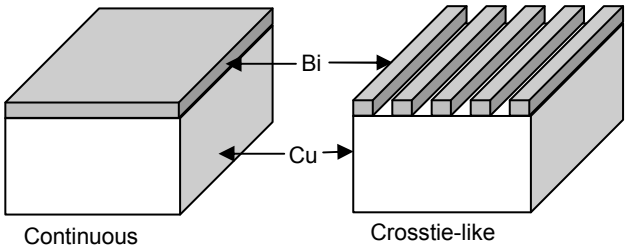

Figure 1. The schemes of continuous and crosstie-like coverage patterns of Bi in a Cu grain boundary.

MODELS

The basic characteristic equation of Auger electron peaks is given as [3]:

$$I = I_0 \Gamma \sigma_i \rho_i \int_0^{\infty} r_i c_i \exp\left(\frac{-z}{\lambda_i}\right) dz . \quad (1)$$

where I_0 is the primary electron intensity, Γ is the analyzer transmission, σ_i is the ionization cross-section of atom i, ρ_i is the probability of the Auger transition, r_i is the backscattering factor, c_i is the concentration of atoms i and λ_i is the mean escape depth of Auger electrons. It can be simplified for standard substances as

$$I_i^{st} = AB_i r_i^{st} c_i^{st} \lambda_i^{st} , \quad (2)$$

where A and B are the element-independent and element-dependent parameters, respectively. Based on Eqs. (1) and (2), the characteristic equations of Auger peaks in two different patterns can be derived.

Pattern I. At first, the Bi coverage on fracture surfaces is considered as a continuous layer which is half of the segregation layer in GBs. If the fracture surface is exposed to air, a continuous adsorption layer forms. This adsorption layer is mainly composed of oxygen and carbon. Assuming a homogeneous distribution of atoms in the layer and an equality of atomic density in the measured and standard samples, the characteristic peaks (I) for Bi, Cu, O and C can be expressed as:

$$I_{Bi} = I_{Bi}^{st} \exp\left(\frac{-z^{ad}}{\lambda_{Bi}^{ad}}\right)\left[1 - \exp\left(\frac{-z^{se}}{\lambda_{Bi}^{se}}\right)\right] \quad (3)$$

$$I_{Cu} = I_{Cu}^{st} \exp\left(\frac{-z^{ad}}{\lambda_{Cu}^{ad}}\right)\exp\left(\frac{-z^{se}}{\lambda_{Cu}^{se}}\right) \quad (4)$$

$$I_O = I_O^{st} \frac{r_O^{ad}\lambda_O^{ad}}{r_O^{st}\lambda_O^{st}} x_O^{ad}\left[1 - \exp\left(\frac{-z^{ad}}{\lambda_O^{ad}}\right)\right] \quad (5)$$

$$I_C = I_C^{st} \frac{r_C^{ad}\lambda_C^{ad}}{r_C^{st}\lambda_C^{st}} \left(1 - x_O^{ad}\right)\left[1 - \exp\left(\frac{-z^{ad}}{\lambda_C^{ad}}\right)\right] \quad (6)$$

The symbols for the thicknesses of the layers of adsorption and segregation are z^{ad} and z^{se}, respectively. One can write the thickness and oxygen concentration in the adsorption layer as:

$$z^{ad} = \frac{\lambda_{Bi}^{ad}\lambda_{Cu}^{ad}}{\lambda_{Bi}^{ad} - \lambda_{Cu}^{ad}} \ln\left\{\frac{I_{Bi}/I_{Bi}^{st}}{I_{Cu}/I_{Cu}^{st}} \frac{\exp\left(\frac{-z^{se}}{\lambda_{Cu}^{se}}\right)}{\left[1 - \exp\left(\frac{-z^{se}}{\lambda_{Bi}^{se}}\right)\right]}\right\}, \quad (7)$$

$$x_O^{ad} = \frac{I_O/I_O^{st}}{I_{Cu}/I_{Cu}^{st}} \frac{r_O^{st}\lambda_O^{st}}{r_O^{ad}\lambda_O^{ad}} \frac{\exp\left(\frac{-z^{se}}{\lambda_{Cu}^{se}}\right)\exp\left(\frac{-z^{ad}}{\lambda_{Cu}^{ad}}\right)}{\left[1 - \exp\left(\frac{-z^{ad}}{\lambda_O^{ad}}\right)\right]} . \quad (8)$$

Using equations (4) to (6), one can get oxygen concentration in the adsorption layer as:

$$x_O^{ad} = \left\{ \frac{I_C / I_C^{st}}{I_O / I_O^{st}} \frac{r_C^{st}\lambda_C^{st}}{r_C^{ad}\lambda_C^{ad}} \frac{r_O^{ad}\lambda_O^{ad}}{r_O^{st}\lambda_O^{st}} \frac{\left[1 - \exp\left(\frac{-z^{ad}}{\lambda_O^{ad}}\right)\right]}{\left[1 - \exp\left(\frac{-z^{ad}}{\lambda_C^{ad}}\right)\right]} + 1 \right\}^{-1} . \quad (9)$$

Pattern II. The segregation layer is fractured into fragments which line up on the surface. The surface can be either covered by pure Bi or be free immediately after fracture. After exposure to air, the thicknesses of adsorption layers on the Bi-covered and free Cu surfaces become different. The total thickness of surface layers including layers of segregation and adsorption is assumed constant. Assuming that the half of the total surface area is covered by a pure Bi segregation layer, the characteristic peaks for Bi, Cu, O and C can be expressed as:

$$I_{Bi} = 0.5 \cdot I_{Bi}^{st} \exp\left[\frac{-\left(z^{ad} - z^{se}\right)}{\lambda_{Bi}^{ad}}\right]\left[1 - \exp\left(\frac{-z^{se}}{\lambda_{Bi}^{se}}\right)\right] \quad (10)$$

$$I_{Cu} = 0.5 \cdot I_{Cu}^{st}\left\{\exp\left[\frac{-\left(z^{ad} - z^{se}\right)}{\lambda_{Cu}^{ad}}\right]\exp\left(\frac{-z^{se}}{\lambda_{Cu}^{se}}\right) + \exp\left(\frac{-z^{ad}}{\lambda_{Cu}^{ad}}\right)\right\}, \quad (11)$$

$$I_O = 0.5 \cdot I_O^{st} \frac{r_O^{ad}\lambda_O^{ad}}{r_O^{st}\lambda_O^{st}} x_O^{ad}\left\{2 - \exp\left(\frac{-z^{ad}}{\lambda_O^{ad}}\right) - \exp\left[\frac{-\left(z^{ad} - z^{se}\right)}{\lambda_O^{ad}}\right]\right\}, \quad (12)$$

$$I_C = 0.5 \cdot I_C^{st} \frac{r_C^{ad}\lambda_C^{ad}}{r_C^{st}\lambda_C^{st}}\left(1 - x_O^{ad}\right)\left\{2 - \exp\left(\frac{-z^{ad}}{\lambda_C^{ad}}\right) - \exp\left[\frac{-\left(z^{ad} - z^{se}\right)}{\lambda_C^{ad}}\right]\right\}. \quad (13)$$

The thickness and oxygen concentration in the adsorbing layer are:

$$z^{ad} = \frac{\lambda_{Bi}^{ad}\lambda_{Cu}^{ad}}{\lambda_{Bi}^{ad} - \lambda_{Cu}^{ad}} \ln\left\{\frac{I_{Bi} / I_{Bi}^{st}}{I_{Cu} / I_{Cu}^{st}} \frac{\left[\exp\left(\frac{-z^{se}}{\lambda_{Cu}^{se}}\right) + \exp\left(\frac{-z^{se}}{\lambda_{Cu}^{ad}}\right)\right]}{\left[1 - \exp\left(\frac{-z^{se}}{\lambda_{Bi}^{se}}\right)\right]}\right\} + z^{se}, \quad (14)$$

$$x_O^{ad} = \frac{I_O / I_O^{st}}{I_{Cu} / I_{Cu}^{st}} \frac{r_O^{st}\lambda_O^{st}}{r_O^{ad}\lambda_O^{ad}}\left\{\frac{\exp\left[\frac{-\left(z^{ad} - z^{se}\right)}{\lambda_{Cu}^{ad}}\right]\left[\exp\left(\frac{-z^{se}}{\lambda_{Cu}^{se}}\right) + \exp\left(\frac{-z^{se}}{\lambda_{Cu}^{ad}}\right)\right]}{2 - \exp\left[\frac{-\left(z^{ad} - z^{se}\right)}{\lambda_O^{ad}}\right] - \exp\left(\frac{-z^{ad}}{\lambda_O^{ad}}\right)}\right\}. \quad (15)$$

Using equations (11) to (13), one can get oxygen concentration in the adsorption layer as:

$$x_O^{ad} = \left\{ \frac{I_C / I_C^{st}}{I_O / I_O^{st}} \frac{r_C^{st}\lambda_C^{st}}{r_C^{ad}\lambda_C^{ad}} \frac{r_O^{ad}\lambda_O^{ad}}{r_O^{st}\lambda_O^{st}} \frac{\left[2 - \exp\left(\frac{-z^{ad}}{\lambda_O^{ad}}\right) - \exp\left(\frac{-\left(z^{ad} - z^{se}\right)}{\lambda_O^{ad}}\right)\right]}{\left[2 - \exp\left(\frac{-z^{ad}}{\lambda_C^{ad}}\right) - \exp\left(\frac{-\left(z^{ad} - z^{se}\right)}{\lambda_C^{ad}}\right)\right]} + 1 \right\}^{-1} . \quad (16)$$

The values of the backscattering factor (r) and mean escape depth of Auger electrons (λ) are

calculated according to the equations below:

$$r_i = \left(0.462 - 0.777Z_i^{0.20}\right)\left(\frac{E_i}{E_0}\right)^{0.32} + \left(1.15Z_i^{0.20} - 1.05\right), \quad (17)$$

$$\lambda_i = 5.38(E_i)^{-2} + 0.41(a_iE_i)^{0.5}\ (\text{ML}), \quad (18)$$

where E_o and E_i are the energies of primary and Auger electrons, Z_i is the atomic number and a_i is the atomic diameter, i= Bi, Cu, O, C.

EXPERIMENTAL

Cu polycrystals (99.999% purity) containing 100 wt. ppm Bi were cast in vacuum. A 15×3×3 mm^3 sample was cut by means of a low-speed diamond saw. The sample was cleaned by acetone and encapsulated. The sample was homogenized at 950°C for 24 hr and then annealed at 675°C for 25 hr. A 0.8 mm deep notch was cut on each long side of this sample for ensuring a complete fracture in the AES apparatus.

The AES instrument used in this work was a PHI 600 Scanning Auger Microprobe. The energy of the primary electron beam was 10 keV. The intensity of Auger electrons was measured by means of a double cylindrical mirror analyzer. At the beginning, the characteristic intensities of Cu and Bi peaks in pure samples were measured as standard. The flat standard samples were 99.999% pure and polished. The Cu–Bi sample was fractured *in-situ* in the analyzing chamber of AES, as it was being cooled with liquid nitrogen. Four points were chosen and noted for analysis on a fracture surface. It was an intergranular fracture. The energy range was 30 to 1000 eV. After acquiring the spectra from the points on the just-fractured surface, the sample was removed from the ultra high vacuum (UHV) chamber and exposed to air for 5 seconds. The exposed sample was then transferred into the UHV chamber and spectra were taken again from the same four points measured previously.

The intensities of Bi and Cu peaks from the as-fractured sample were measured. From the sample exposed to air the intensities of Bi, Cu, C and O peaks were measured. The resultant data were put into the corresponding equations of characteristic intensity of Auger electron peaks for quantification. Taking pattern I as an example, the value of the thickness of segregation layer was increased from 0 in a step of 0.01 monolayer and inserted into Eq. (7) to calculate the thickness of the adsorption layer. Both thicknesses of the segregation and adsorption layers were inserted into Eqs. (8) and (9). The values calculated via both equations were compared and when the difference between them was at the minimum, the corresponding value of the thickness of the segregation layer was recorded as the final result.

RESULTS AND DISCUSSION

Figure 2 shows one of the AES spectra obtained in this study. Only Cu and Bi peaks are present in the sample just fractured, while C and O peaks additionally appear in the sample exposed to air. It should be noted that only the segregation layer covers the surface of the sample just fractured and both the layers of adsorption and segregation exist on the surface of the sample exposed in air. It can be seen that the relative intensity of the Cu peak to the Bi peak is lowered after exposure to air. This is caused by the lengthening of the escaping path needed for Auger electrons induced below the adsorption layer and this effect is more pronounced for Cu than for Bi because the latter lies closer to the topmost surface.

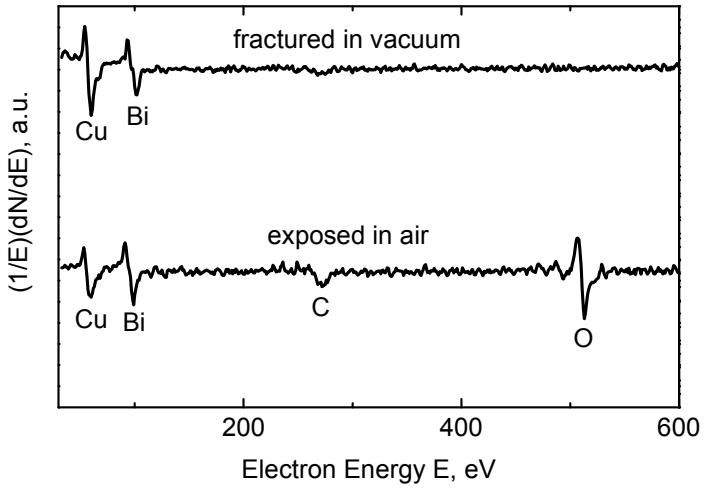

Figure 2. AES spectra obtained in this study. Only Cu and Bi peaks are present in the sample just fractured, while C and O peaks additionally appear in the sample exposed to air.

The thicknesses of the segregation layer of Bi in the polycrystalline Cu calculated based on the fracture patterns I and II are listed in Table 1. These data are also shown as a diagram in Figure 3. It is found that for the as-fractured sample the value (2.35 ML) of the thickness of segregation layer at the GB quantified from the patterns I dose not deviate much from that (2.15 ML) quantified from the pattern II. After exposing the sample in air, the value of the thickness of segregation layer quantified from the pattern I drastically changes to 3.43 ML with a 46% increase. By contrast, the value (2.52 ML) quantified from the pattern II shows only a 17% increase.

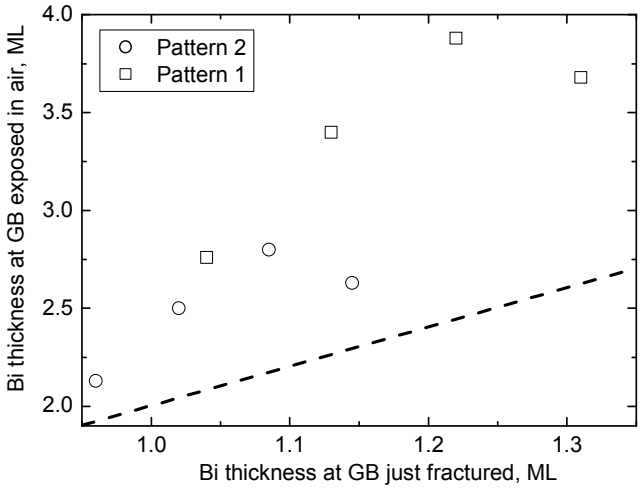

Figure 3. The thicknesses of the segregation layer of Bi in the polycrystalline Cu calculated based on the fracture patterns I and II (Table 1).

The dashed line in Figure 3 is the line of equal values of the thickness of segregation layer at the GB just fractured and exposed in air. The data from the pattern II lie closer to the dashed line and therefore exhibit better agreement. From this evidence, it can be stated fairly emphatically that

the coverage pattern on the fracture surface of Bi-embrittled Cu grain boundaries is a crosstie-like pattern.

Table 1. Thicknesses of the segregation layer calculated based on the fracture patterns I and II.

Point no.	Bi Thickness from Pattern I, ML		Bi thickness from Pattern II, ML	
	fractured	exposed in air	fractured	exposed in air
1	2.08	2.76	1.92	2.13
2	2.26	3.4	2.04	2.50
3	2.44	3.88	2.17	2.80
4	2.62	3.68	2.29	2.63
average	2.35	3.43	2.10	2.52

ACKNOWLEDGEMENT

This work was financially supported by the Russian Foundation for Basic Research under the contract 05-03-90578 and National Scientific Council of Taiwan under the contracts RP05E14 and NSC 94-2218-E-005-015.

REFERENCES

[1] L.-S. Chang, E. Rabkin, B.B. Straumal, B. Baretzky and W. Gust: Acta Mater. Vol. 47 (1999), p. 4041.

[2] W. Siegle, L.-S. Chang and W. Gust: Phil. Mag. A Vol. 82 (2002), p. 1595.

[3] D. Briggs and M.P. Seah: *Practical Surface Analysis*, 2nd Edition, John Wiley & Sons, London, 1990, p. 208.